Fast-particle energy loss in the vicinity of a two-dimensional plasma

N. J. M. Horing and H. C. Tso
Department of Physics, Stevens Institute of Technology, Hoboken, New Jersey 07030

Godfrey Gumbs
Department of Physics, University of Lethbridge, Lethbridge, Alberta, Canada T1K 3M4
(Received 28 July 1986; revised manuscript received 6 February 1987)

This paper presents an analysis of the energy loss of a fast-charged-particle probe of a two-dimensional (2D) collisionless solid-state plasma. The fast-particle motion is taken to be parallel to the 2D plasma sheet, and the plasma is taken to be in a degenerate state (zero temperature). The 2D plasma response dynamics are described in the random-phase approximation (RPA), and our calculation is a 2D analogue of the well-known Nozières-Pines energy-loss calculation, but with the particle's trajectory at a fixed distance H from the plane of the 2D plasma sheet. Our calculation includes a determination of the part of the fast particle's energy loss which can be ascribed to the excitation of electron-hole pairs in the 2D plasma, as well as the part which can be ascribed to 2D plasmons (of all wave numbers). We determine the energy loss as a function of the distance of the fast particle from the 2D plasma plane, and its velocity.

I. INTRODUCTION

The interaction of a fast-charged particle with a medium has proven to be an important probe of the properties of matter. Moreover, the intense focus of concern on surface physics in recent years has spurred investigations of charged particles interacting with bounded media. Our interest here is to analyze the energy-loss rate of a fast-charged particle passing parallel to a planar sheet of two-dimensional (2D) solid-state plasma, whose dynamics are described by the random-phase approximation (RPA). For example, this analysis is applicable to a semiconductor inversion layer.[1] Our "dielectric formulation" for the energy-loss rate will be set up in a way that is easily extended to other bounded systems (as well as unbounded systems) for which the inversion of the dielectric function can be carried out, and it closely parallels other recent work.[2] It has already been employed in the analysis of energy loss to a semi-infinite medium[3] to determine the effects of an ambient quantizing magnetic field.[4] In regard to the problem of energy loss to a 2D plasma sheet of interest here, our work differs from the corresponding analysis of Fetter[2(a)] in that we employ an RPA description of the 2D plasma in contrast to his hydrodynamic model of plasma dynamics. Even so, some of our results are identical with those of Fetter. In particular, for very high velocity one should expect nonlocal shielding to be ineffective (as there is not enough time for a static redistribution of charge to take place) and so the local 2D plasmon structure of dielectric response should determine the energy-loss rate. Since the local 2D plasmon limit of response is identical in the RPA and in the hydrodynamic model, it is clear that the high-velocity energy-loss rate which we will determine will be the same as that of Fetter. It is at lower velocities that significant differences should occur as the transfer of energy to particle-hole excitations becomes more important, and to examine this we carry out an explicit analytic determination of the stopping power of a 2D plasma to linear order in (low) velocity, and we also do a numerical RPA evaluation of 2D energy loss at arbitrary (intermediate) velocities, in all cases examining the dependence of the energy-loss rate on the distance H of the passing charged particle from the plane (to which it is in parallel motion).

II. DIELECTRIC FORMULATION OF ENERGY LOSS

Our formulation of the energy loss of a fast particle moving parallel to a sheet of two-dimensional (2D) plasma in the (x-y) plane proceeds from the observation that the fast particle moving with velocity $\mathbf{v}=v\hat{\mathbf{i}}$ parallel to the plane impresses a Coulomb potential $U(2)$ at a space-time point $2=(\mathbf{r}_2,t_2)$ which is dynamically screened by the 2D plasma. (Only electrostatic interactions are considered here.) The resulting effective potential $V(1)$ at a space-time point $1=(\mathbf{r}_1,t_1)$ is given by

$$V(1)=\int d^4 2K(1,2)U(2) , \tag{1}$$

where $K(1,2)$ is the inverse dielectric function for the 2D plasma in a 3D real space-time representation such that

$$\int d^4 3K(1,3)\epsilon(3,2)=\delta^4(1,2) ,$$

and $\epsilon(3,2)$ is the direct dielectric function of the 2D plasma in 3D real space-time representation. One must also recognize that there is a density perturbation involved in the response dynamics, such that

$$\rho(1)=\int d^4 3R(1,3)V(3) = \int d^4 3\int d^4 4\, R(1,3)K(3,4)U(4) \tag{2}$$

with $R(1,3)=\delta\rho(1)/\delta V(3)$ as the density-perturbation response function. Employing the random-phase-approximation (RPA) integral equation

$$K(1,2)=\delta^4(1-2)-\int d^43\,\alpha(1,3)K(3,2)\ , \tag{3a}$$

we write the polarizability $\alpha(1,3)$ in a form which describes both the free-electron response and an additive static background contribution (v_c is the interelectron Coulomb interaction of the plasma, and $\alpha_0=\epsilon_0-1$ is the additive background polarizability):

$$\alpha(1,3)=-\int d^44\,v_c(1-4)R(4,3)+\alpha_0\delta^4(1-3)\ . \tag{3b}$$

This yields

$$K(1,2)=\frac{1}{\epsilon_0}\delta^4(1-2)+\frac{1}{\epsilon_0}\int d^43\int d^44\,v_c(1-4)R(4,3)K(3,2)\ ,$$

and consequently

$$\nabla_1^2[K(1,2)-\delta^4(1-2)/\epsilon_0]=\frac{-4\pi e}{\epsilon_0}\int d^43\,R(1,3)K(3,2) \tag{4}$$

which permits $\rho(1)$ to be rewritten as

$$\rho(1)=-\frac{\epsilon_0}{4\pi e}\int d^44\,\nabla_1^2[K(1,4)-\delta^4(1-4)/\epsilon_0]U(4)\ . \tag{5}$$

Since the force on an element of plasma is $-e\rho(1)\nabla_1V(1)$, the reaction force of a frictional nature on the fast particle is given by

$$\mathbf{f}=e\int d^31\,\rho(1)\nabla_1V(1)\ , \tag{6}$$

and the rate at which the fast particle loses energy is $\mathbf{f}\cdot\mathbf{v}=vf_x$. Our calculations proceed from Eq. (6) jointly with Eq. (1) and Eq. (5). Considering translational invariance in the $\bar{r}=(x,y)$ plane and time (but not for z) we Fourier transform

$$K(1,2)=K(\bar{r}_1-\bar{r}_2,z_1,z_2;t_1-t_2)\to K(\bar{p},z_1,z_2;\omega)$$

with respect to space $\bar{r}_1-\bar{r}_2\to\bar{p}$ and time $t_1-t_2\to\omega$. The inverse dielectric function $K(\bar{p},z_1,z_2;\omega)$ for a 2D plasma sheet in 3D space is readily determined as[5] (see the Appendix).

$$K(\bar{p},z_1,z_2;\omega)-\frac{\delta(z_1-z_2)}{\epsilon_0}=\frac{\delta(z_2)}{\epsilon_0}e^{-p|z_1|}[\tilde{K}^{2D}(\bar{p},\omega)-1]\ , \tag{7}$$

where $\tilde{K}^{2D}(\bar{p},\omega)$ is the 2D inverse dielectric function on the 2D plane, algebraically $\tilde{K}^{2D}(\bar{p},\omega)=1/\tilde{\epsilon}^{2D}(\bar{p},\omega)$, with background shielding incorporated by means of $v_c\to\bar{v}_c=v_c/\epsilon_0$ or $e^2\to\tilde{e}^2=e^2/\epsilon_0$. Moreover, the impressed Coulomb potential $U(2)$ of the fast particle (charge strength Ze) moving parallel to the surface and at a height H above it has the form

$$U(2)=Ze\,|\mathbf{r}_2-vt_2\hat{\mathbf{i}}-H\hat{\mathbf{k}}|^{-1}\ .$$

These considerations determine the energy loss per unit time as ($\tilde{e}^2\equiv e^2/\epsilon_0$)

$$\frac{dW}{dt}=\mathbf{f}\cdot\mathbf{v}=-Z^2\tilde{e}^2v\int\frac{d^2\bar{p}}{2\pi}\frac{ip_x}{p}\tilde{K}^{2D}(\bar{p},-\bar{p}\cdot\bar{v})\times[\tilde{K}^{2D}(-\bar{p},\bar{p}\cdot\bar{v})-1]e^{-2pH}\ . \tag{8}$$

In view of the fact that[6] both the real and imaginary parts of $\tilde{K}^{2D}(\bar{p},\omega)$ are even functions of $\bar{p}$, whereas the real part is even in ω but the imaginary part is odd in ω, the $\tilde{K}^{2D}\tilde{K}^{2D}$ term of Eq. (8) may be seen to have an odd p_x integrand leading to a null result. The remaining $\tilde{K}^{2D}$ term has its real part vanish for the same reason, and consequently the result involves the imaginary part of $\tilde{K}^{2D}$ alone:

$$\frac{dW}{dt}=-Z^2\tilde{e}^2v\int\frac{d^2\bar{p}}{2\pi}e^{-2pH}\frac{p_x}{p}\,\mathrm{Im}\tilde{K}^{2D}(\bar{p},-\bar{p}\cdot\bar{v})\ . \tag{9}$$

Alternatively, one may express this in the equivalent form

$$\frac{dW}{dt}=\frac{-Z^2\tilde{e}^2}{2\pi v}\int_{-\infty}^{\infty}dp_y\int_{-\infty}^{\infty}d\omega\frac{\omega}{p}e^{-2pH}\times\mathrm{Im}\tilde{K}^{2D}(\bar{p},-\omega) \tag{10}$$

with

$$p\to\left[p_y^2+\left[\frac{\omega}{v}\right]^2\right]^{1/2}$$

and

$$\mathrm{Im}\tilde{K}^{2D}(\bar{p},-\omega)=-\tilde{\epsilon}_2^{2D}(\bar{p},\omega)/[\tilde{\epsilon}_1^{2D}(\bar{p},\omega)^2+\tilde{\epsilon}_2^{2D}(\bar{p},\omega)^2]$$

where

$$(\tilde{K}^{2D})^{-1}=\tilde{\epsilon}^{2D}=\tilde{\epsilon}_1^{2D}+i\tilde{\epsilon}_2^{2D}$$

is written in terms of the real and imaginary parts of the two-dimensional RPA dielectric function determined by Stern[7] as follows for zero temperature:

$$\tilde{\epsilon}_1^{2D}(\bar{p},\omega)=1+\frac{2\tilde{e}^2m^2}{\hbar^3p^3}\left\{\frac{\hbar p^2}{m}-\sum_{\pm}\mathrm{sgn}\left[\frac{\hbar p^2}{2m}\pm\omega\right]\eta_+\left[\left[\frac{\hbar p^2}{2m}\pm\omega\right]^2-\frac{2p^2\zeta}{m}\right]\left[\left[\frac{\hbar p^2}{2m}\pm\omega\right]^2-\frac{2p^2\zeta}{m}\right]^{1/2}\right\}\ , \tag{11a}$$

$$\tilde{\epsilon}_2^{2D}(\bar{p},\omega)=\frac{2\tilde{e}^2m^2}{\hbar^3p^3}\sum_{\pm}(\pm)\eta_+\left[\frac{2p^2\zeta}{m}-\left[\frac{\hbar p^2}{2m}\mp\omega\right]^2\right]\left[\frac{2p^2\zeta}{m}-\left[\frac{\hbar p^2}{2m}\mp\omega\right]^2\right]^{1/2}\ . \tag{11b}$$

Here, ζ is the Fermi energy, m, $\tilde{e}=e/\sqrt{\epsilon_0}$ are the electron effective mass and charge, respectively, and $\eta_+(x)$ is the Heaviside unit-step function. Hereafter we suppress explicit reference to the overhead tilde, and understand that $e^2 \to e^2/\epsilon_0$ everywhere.

III. LOW- AND HIGH-VELOCITY LIMITS AND LARGE-DISTANCE (H) LIMIT

A. Low velocity

The low-velocity limit is of special interest, and in this case we may expand

$$K^{2D}(\bar{p},-\bar{p}\cdot\bar{v}) \cong K^{2D}(\bar{p},0) - \frac{\partial K^{2D}}{\partial \omega}(\bar{p},\omega=0)p_x v \ .$$

The first term gives a null contribution to $dW/dt = \mathbf{f}\cdot\mathbf{v}$ since the p_x integrand is odd. The second term yields

$$\frac{dW}{dt} \cong Z^2 e^2 v^2 \int \frac{d^2\bar{p}}{2\pi} e^{-2pH}\frac{p_x^2}{p}\,\mathrm{Im}\left[\frac{\partial K^{2D}}{\partial\omega}(\bar{p},\omega=0)\right]$$
$$\cong -Z^2e^2v^2\int_0^\infty dp\,\tfrac{1}{2}e^{-2pH}p^2 \times \frac{\partial\epsilon_2^{2D}(\bar{p},\omega=0)}{\partial\omega}\Big/[\epsilon_1^{2D}(\bar{p},0)]^2 \ , \tag{12}$$

since $\epsilon_2^{2D}(\bar{p},\omega=0)$ and $(\partial/\partial\omega)\epsilon_1^{2D}(\bar{p},\omega=0)$ vanish as odd functions of ω. Direct calculation based on Eq. (11) yields

$$\frac{dW}{dt} = -\frac{2Z^2e^4m^2v^2}{\hbar^3}\int_0^{2p_F} dp \frac{e^{-2pH}}{[(2p_F)^2-p^2]^{1/2}} \times \left[1+\frac{2e^2m}{\hbar^2 p}\right]^{-2} , \tag{13}$$

where p_F is the Fermi wave number. Considering the Bohr radius $a_0 \sim \hbar^2/me^2$ to be the smallest length of the system ($a_0 \ll H, p_F^{-1}$), the corresponding stopping power $dW/dl = v^{-1}dW/dt$ is given by

$$\frac{dW}{dl} = -\frac{Z^2\hbar v}{8}\frac{\partial^2}{\partial H^2}\int_0^{2p_F} dp \frac{e^{-2pH}}{[(2p_F)^2-p^2]^{1/2}} \ . \tag{14}$$

The result of integrating equation (14) may be expressed[8] in terms of modified Bessel functions $I_n(x)$ (first kind) and modified Struve functions $L_n(x)$;

$$\frac{dW}{dl} = -\pi Z^2\hbar p_F^2 v\left[[I_2(4p_FH)-L_2(4p_FH)]+[I_1(4p_FH)-L_1(4p_FH)]/4p_FH - \frac{8p_FH}{3\pi}\right] . \tag{15}$$

It should be noted that this result is valid under the condition $a_0 \ll p_F^{-1}$ alone (irrespective of the value of a_0/H) for all values of p_FH. For the special cases of $4p_FH \ll 1$ and $4p_FH \gg 1$, we obtain

$$\frac{dW}{dl} = \begin{cases} \dfrac{-\pi\hbar p_F^2 Z^2 v}{2} & \text{for } 4p_FH \ll 1 \quad (p_Fa_0 \ll 1) \ , \\[2ex] \dfrac{-Z^2\hbar p_F v}{2H} & \text{for } 4p_FH \gg 1 \quad (p_Fa_0 \ll 1) \ . \end{cases}$$

On the other hand, for a high-density 2D plasma (sheet density ρ^{2D}) we have $p_Fa_0 = (2\pi\rho^{2D})^{1/2}a_0 \gg 1$ and corresponding to this Eq. (13) yields

$$\frac{dW}{dl} = -\frac{2Z^2e^4m^2v}{\hbar^3}\int_0^{2p_F} dp\, e^{-2pH}\Big/[(2p_F)^2-p^2]^{1/2} \ , \tag{16}$$

whence

$$\frac{dW}{dl} = -\frac{\pi Z^2e^4m^2v}{\hbar^3}[I_0(4p_FH)-L_0(4p_FH)] \ . \tag{17}$$

The special cases of $4p_FH \ll 1$ and $4p_FH \gg 1$ are given by

$$\frac{dW}{dl} = \begin{cases} \dfrac{-\pi Z^2e^4m^2v}{\hbar^3} & \text{for } 4p_FH \ll 1 \quad (p_Fa_0 \gg 1) \ , \\[2ex] \dfrac{-Z^2e^4m^2v}{2\hbar^3 p_FH} & \text{for } 4p_FH \gg 1 \quad (p_Fa_0 \gg 1) \ . \end{cases}$$

B. High velocity

The high-velocity limit is also amenable to analysis, since in this case the frequency argument $\omega = -p_xv$ of $K^{2D}(\bar{p},-\bar{p}\cdot\bar{v})$ in Eq. (9) is so large in relation to relevant wave-number parameters that we may employ the local "2D plasmon" limit for dielectric response (Δ is an infinitesimal positive number)

$$K^{2D}(\bar{p},-\bar{p}\cdot\bar{v}) \to -K^{2D}(0,\bar{p}\cdot\bar{v}) = -\left[1-\frac{2\pi e^2\rho^{2D}p}{m(\omega+i\Delta)^2}\right]^{-1}_{\omega=p_xv} \tag{18a}$$

and

$$\mathrm{Im}K^{2D}(\bar{p},-\bar{p}\cdot\bar{v}) = \pi\delta(1-2\pi e^2\rho^{2D}p/m\omega^2)_{\omega=p_xv}\,\mathrm{sgn}(p_x) \ . \tag{18b}$$

Thus, for high velocity we have (in 2D polar coordinates)

$$\frac{dW}{dt} = -2Z^2e^2\int_0^\infty dp\,pe^{-2pH}\int_0^{\pi/2} d\theta\cos\theta\,\delta(1-2\pi e^2\rho^{2D}/mv^2p\cos^2\theta) \tag{19}$$

and the Dirac δ function of Eq. (19) is given by

$$\delta(\cdots)=\tfrac{1}{2}\eta_+(p-2\pi e^2\rho^{2D}/mv^2)\times\left[\frac{\cos^2\theta_0}{1-\cos^2\theta_0}\right]^{1/2}\delta(\theta-\theta_0)\ ,$$

where $\cos^2\theta_0=2\pi e^2\rho^{2D}/mv^2p$ for $\pi/2\geq\theta_0\geq 0$. Executing the θ integral we have

$$\frac{dW}{dt}=\frac{\pi Z^2e^4\rho^{2D}}{mv}\frac{\partial}{\partial H}\times\int_{(2\pi e^2\rho^{2D}/mv^2)}^{\infty}dp\,e^{-2pH}\Big/\left[p\left[p-\frac{2\pi e^2\rho^{2D}}{mv^2}\right]\right]^{1/2}\tag{20}$$

which may be evaluated in terms of modified Bessel (Whittaker) functions[9] $K_n(x)$,

$$\frac{dW}{dt}=\frac{-2\pi^2Z^2e^6(\rho^{2D})^2}{m^2v^3}e^{-(2\pi e^2\rho^{2D}H/mv^2)}\times\left[K_0\left[\frac{2\pi e^2\rho^{2D}H}{mv^2}\right]+K_1\left[\frac{2\pi e^2\rho^{2D}H}{mv^2}\right]\right]\ .\tag{21}$$

That this result is consistent with that of Fetter[2(a)] (corresponding to his result for v much greater than the Fermi velocity v_F should be no surprise since his hydrodynamic analysis describes the same local 2D plasmon dynamics which characterize our high-velocity dielectric response in the RPA analysis here. Both results diverge as $H\to 0$, as one can readily see from Eq. (20) as $v\to\infty$, yielding

$$\left|\frac{dW}{dt}\right|=\frac{\pi Z^2e^4\rho^{2D}}{mvH}\ .\tag{22}$$

This divergence as $H\to 0$ is a consequence of the fact that our 2D plasma sheet has zero width, and we have verified that the inclusion of a finite width b yields a convergent result as $z\to 0$—but reproduces Eq. (22) for very high velocity provided that $z>b$. Thus, for distances z greater than the width of the 2D sheet, the present zero-width analysis is valid and meaningful.

C. Large-distance (H) limit

In the case when the distance H is the dominantly large distance in the analysis, we note that the energy loss given by Eq. (9) is mainly governed by low wave-number contributions (e^{-2pH} factor) so that the dielectric response is effectively determined by the local 2D plasmon limit $K^{2D}(0,\bar{p}\cdot\bar{v})$. Accordingly, Eqs. (21) and (22) pertain to this large-distance limit quite generally.

IV. NUMERICAL EVALUATION FOR ARBITRARY VELOCITY

For arbitrary velocity it is necessary to undertake a numerical evaluation of the RPA energy-loss rate. Employing Eq. (9) in 2D polar coordinates (p,θ) and setting $x=\cos\theta$, we have

$$\left|\frac{dW}{dt}\right|=\frac{2Z^2e^2v}{\pi}\int_0^{\infty}dp\,pe^{-2pH}\int_0^1dx\frac{x}{(1-x^2)^{1/2}}\frac{\epsilon_2^{2D}(p,pvx)}{[\epsilon_1^{2D}(p,pvx)]^2+[\epsilon_2^{2D}(p,pvx)]^2}\ .\tag{23}$$

The Heaviside unit-step functions of Eq. (11b) for $\epsilon_2^{2D}(\bar{p},\omega)$ determine cutoffs for the vanishing of ϵ_2^{2D} within which the contribution to energy loss may be attributed to particle-hole excitations. However, it must be recognized that a nonlocal 2D plasmon-pole contribution will enter when ϵ_2^{2D} vanishes if ϵ_1^{2D} vanishes as well, for in this case

$$\epsilon_2^{2D}/[(\epsilon_1^{2D})^2+(\epsilon_2^{2D})^2]\to\pi\delta(\epsilon_1^{2D})\ .$$

Thus we classify the types of contributions as particle-hole (p-h) and plasmon (pl)

$$\frac{dW}{dt}=\frac{dW_{p\text{-}h}}{dt}+\frac{dW_{\rm pl}}{dt}\ .\tag{24}$$

The limits of integration for $dW_{p\text{-}h}/dt$ are determined by the zeros of

$$\left[\frac{2p^2\zeta}{m}-\left[\frac{\hbar p^2}{2m}\mp pvx\right]^2\right]=0\tag{25}$$

(considered jointly with the limits of the x integral [0,1]).

The nonlocal plasmon contribution takes the form

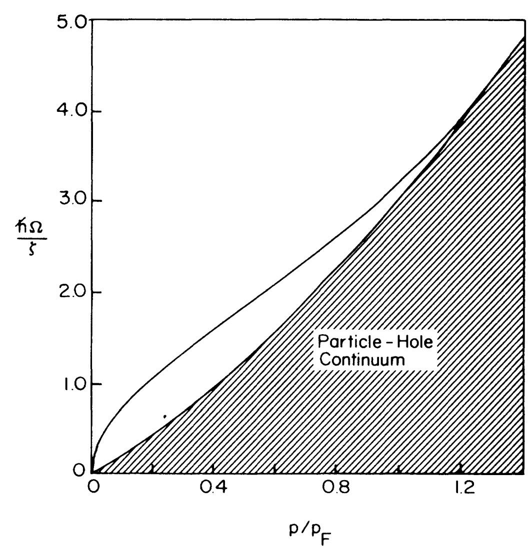

FIG. 1. Plot of two-dimensional plasmon dispersion relation and particle-hole excitations as functions of wave number. The values of the material parameters are presented in the text.

$$\frac{dW_{\rm pl}}{dt}=2Z^2e^2v\int_0^{p_{\max}}dp\,pe^{-2pH}\int_0^1 dx\frac{x}{(1-x^2)^{1/2}}\left[\frac{\delta(\omega-\omega_0)}{\left|\frac{d\epsilon_1^{2D}(p,\omega)}{d\omega}\right|}\right]_{\omega=pvx}, \tag{26}$$

where ω_0 is the nonlocal plasmon root of $\epsilon_1^{2D}(\omega_0)=0$, $x_0=\omega_0/pv$, and $p_{\max}$ represents the maximum wave number for an undamped plasmon. The spectrum of 2D plasmon and particle-hole excitations is shown in Fig. 1, and $p_{\max}$ is represented by the intersection of the 2D plasmon curve with the particle-hole continuum. The values of the material parameters employed are appropriate for a (100) p-type Si inversion-layer system with $\epsilon_0=12$, $m=0.2m_e$, $\rho^{2D}=10^{12}$ cm^{-2}. The Fermi wave number is $p_F=0.0251$ Å^{-1} and the Fermi velocity is 1.45×10^7 cm/sec. In Fig. 2, the plasmon and particle-hole contributions to the energy loss are plotted as functions of the impinging projectile velocity for various distances above the 2D plasma plane. These results were obtained from Eq. (10) jointly with Eqs. (24)–(26), by employing the full RPA dielectric function given by Eq. (11). It is of interest to note that the numerical results indicate dominance of the plasmon contribution at large distances

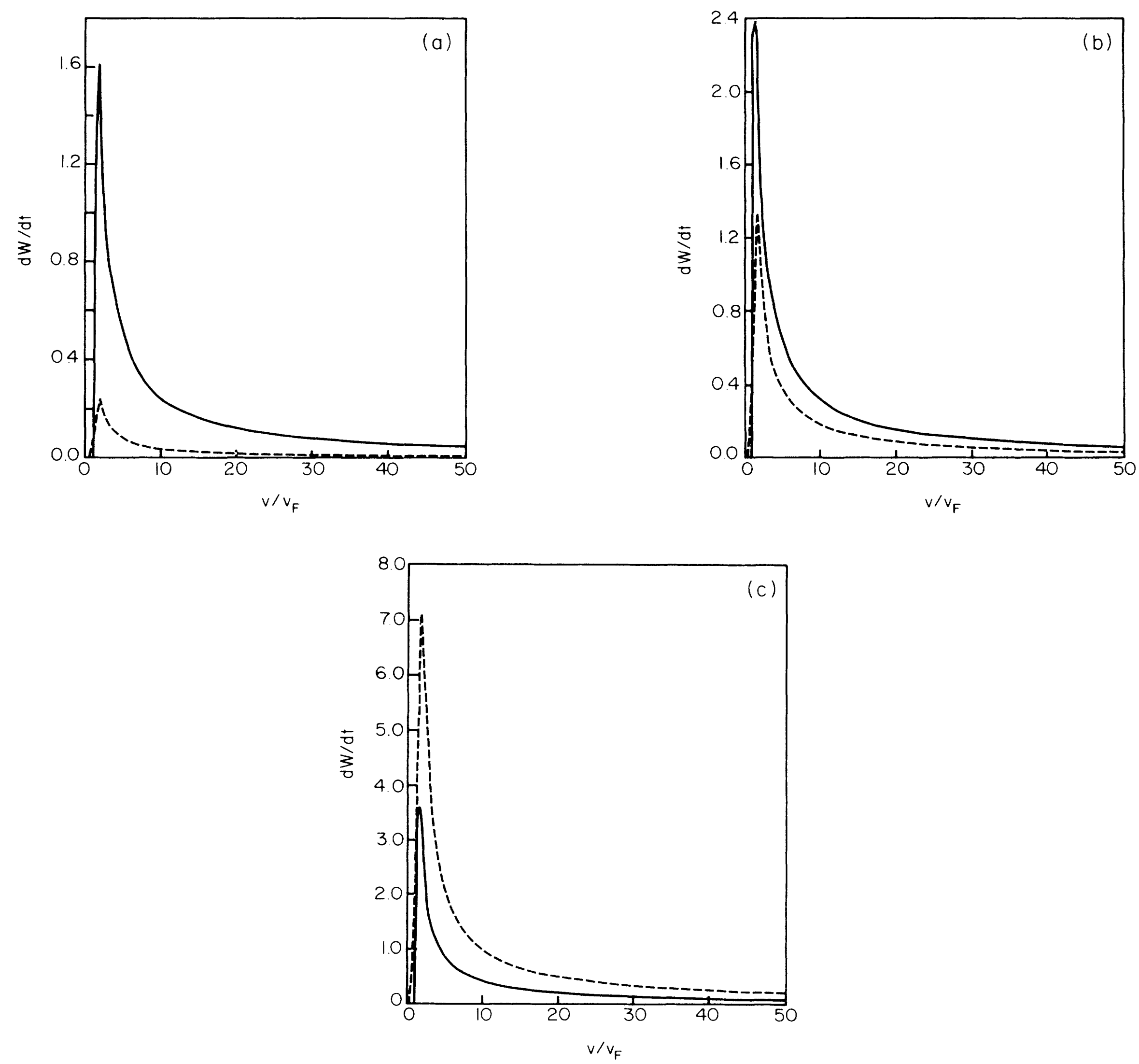

FIG. 2. The energy loss in units of $(Z\zeta)^2/\hbar$ is plotted as a function of the fast particle velocity v in units of v_F. The contributions due to the particle-hole excitations (dashed curves) and plasmon modes (solid curves) are shown for various distances H from the 2D plasma sheet. (a) $H=p_F^{-1}$, (b) $H=0.5p_F^{-1}$, and (c) $H=0.1p_F^{-1}$.

in Fig. 2(a) ($H=p_F^{-1}$) and Fig. 2(b) ($H=0.5p_F^{-1}$), as expected from our analytical studies above. However, for shorter distances as represented in Fig. 2(c) ($H=0.1p_F^{-1}$), the particle-hole contribution is larger than the plasmon contribution; nevertheless, it is to be expected that even in this case the plasmon contribution will become more prominent at very high velocities beyond the scale of Fig. 2(c).

Although nonlocality (spatial dispersion) in the dominant plasmon contribution is insignificant for the extremes of high velocity v and/or large distance H [nonlocality parameters

$$p^2\zeta/m\omega^2 \to p^2\zeta/mp^2v^2 \to (v_F/v)^2 \ll 1$$

and $p/p_F \sim H^{-1}/p_F \ll 1$], the more moderate ranges of velocity and/or distance bear significant nonlocal corrections, particularly through the contributions of particle-hole excitations which are clearly in evidence in Figs. 2(a)–2(c). Such nonlocal spatial-dispersion particle-hole contributions are in fact larger than the plasmon contribution in Fig. 2(c) even at $v \sim 50v_F$ for $H=0.1p_F^{-1}$. In Fig. 2(b) such nonlocal contributions are smaller than that of the plasmon, but exceed 50% of the plasmon part in general for $H=0.5p_F^{-1}$. Nonlocality is smaller still relative to the plasmon in Fig. 2(a) for $H=p_F^{-1}$, but it is still significant and cannot be ignored. It should also be noted that in the low-velocity (linear) regime, nonlocality is always dominant since screening goes into the static limit, as in Eq. (12) for example.

ACKNOWLEDGMENT

One of us (N.J.M.H.) was partially supported by the U.S. Army, Electronic Materials Research Division at the Electronics Technology and Devices Laboratory, Fort Monmouth, N.J., and one of us (G.G.) was partially supported by the Natural Sciences and Engineering Research Council of Canada.

APPENDIX

To determine the inverse of the 2D plasma dielectric function $\epsilon(\bar{p},z_1,z_2;\omega)$ in 3D space, we employ arguments similar to those of Ref. 5. The inversion condition,

$$\int dz_2 K(\bar{p},z_1,z_2;\omega)\epsilon(\bar{p},z_2,z_3;\omega)=\delta(z_1-z_3)\ , \qquad \text{(A1)}$$

may be applied to Eq. (3a) to write $\epsilon(\bar{p},z_1,z_2;\omega)$ as

$$\epsilon(\bar{p},z_1,z_2;\omega)=\delta(z_1-z_2)+\alpha(\bar{p},z_1,z_2;\omega)\ . \qquad \text{(A2)}$$

$\alpha(\bar{p},z_1,z_2;\omega)$ is given by Eq. (3b), and we note that for electron motion confined to a single 2D plane sheet, the density-perturbation response function has its z arguments localized to the sheet by positional δ functions of the form

$$R(\bar{p},z_1,z_2;\omega)=\delta(z_1)\delta(z_2)R^{2D}(\bar{p},\omega)\ . \qquad \text{(A3)}$$

Here, $R^{2D}(\bar{p},\omega)$ describes the electron density perturbation response properties on the 2D sheet, such that the 2D electron polarizability on the sheet is given by $\alpha^{2D}(\bar{p},\omega)=-R^{2D}(\bar{p},\omega)/p$. With this in view, we find that Eq. (3b) and Eqs. (A2) and (A3) jointly yield

$$\epsilon(\bar{p},z_1,z_2;\omega)=\epsilon_0\delta(z_1-z_2)+\delta(z_2)\alpha^{2D}(\bar{p},\omega)e^{-p|z_1|}\ , \qquad \text{(A4)}$$

where $p=|\bar{p}|$ and $\epsilon_0=1+\alpha_0$ for the background. Guided by the experience of Ref. 5, we attempt inversion in the form

$$K(\bar{p},z_1,z_2;\omega)=\frac{1}{\epsilon_0}\delta(z_1-z_2) + \frac{1}{\epsilon_0}\delta(z_2)e^{-p|z_1|}[\tilde{K}^{2D}(\bar{p},\omega)-1]\ . \qquad \text{(A5)}$$

The determination of $\tilde{K}^{2D}(\bar{p},\omega)$ is carried out by requiring satisfaction of the inversion condition in the form of Eq. (A1): Equating coefficients of like positional delta functions, we obtain

$$\tilde{K}^{2D}(\bar{p},\omega)=\left[1+\frac{\alpha^{2D}(\bar{p},\omega)}{\epsilon_0}\right]^{-1}\equiv[\tilde{\epsilon}^{2D}(\bar{p},\omega)]^{-1}\ . \qquad \text{(A6)}$$

$\alpha^{2D}(\bar{p},\omega)$ was determined by Stern[7] for null magnetic field and division by ϵ_0 corresponds to putting $v_c \to \tilde{v}_c = v_c/\epsilon_0$ or $e^2 \to \tilde{e}^2 = e^2/\epsilon_0$. A simple example of the utility of Eq. (A5) is provided in the determination of the statically screened Coulomb potential sited at $(0,0,z_0)$ in 3D space, with the electron sheet on the 2D plane $z=0$: Taking $\epsilon_0 \to 1$, we have the shielded potential as

$$V(\mathbf{r},t\to\infty)=\int\frac{d^2\bar{p}}{(2\pi)^2}e^{i\bar{p}\cdot\bar{r}}\int dz'K(\bar{p},z,z';\omega\to 0)e^{-p|z'-z_0|}/p$$
$$=\int\frac{d^2\bar{p}}{(2\pi)^2}\frac{e^{i\bar{p}\cdot\bar{r}}}{p}\left[e^{-p|z-z_0|}-e^{-p(|z|+|z_0|)}\frac{\alpha^{2D}(\bar{p},\omega\to 0)}{1+\alpha^{2D}(\bar{p},\omega\to 0)}\right]\ . \qquad \text{(A7)}$$

For a perfect metal sheet $\alpha^{2D}\to-\infty$, this yields a perfect image field of relative strength -1 on the same side of the sheet as the Coulomb site (same sign for z,z_0); and also it yields a completely shielded null result at points on the other side of the sheet (different signs for z,z_0) as one should expect.

[1]A thorough review of 2D electron systems is given by T. Ando, A. Fowler, and F. Stern, Rev. Mod. Phys. **54**, 437 (1982).

[2](a) A. L. Fetter, Ann. Phys. (N.Y.) **81**, 367 (1973); (b) B. N. J. Persson and J. E. Demuth, Phys. Rev. B **30**, 5968 (1984); (c) Y. Goldstein *et al.*, Surf. Sci. **98**, 599 (1980); (d) A. Many *et al.*, *ibid.* **113**, 355 (1982); (e) J. J. Ritsko and M. J. Rice, Phys. Rev. Lett. **42**, 666 (1979).

[3](a) T. L. Ferrell, P. M. Echenique, and R. H. Ritchie, Solid State Commun. **32**, 419 (1979); (b) A. A. Lucas and M. Sonjic, Phys. Rev. Lett. **26**, 229 (1971); (c) A. A. Lucas and E. Kartheuser, Phys. Rev. **B1**, 3588 (1970).

[4]G. Gumbs, N. J. M. Horing, S. Silverman, and H. C. Tso, *Proceedings of the 2nd International Conference on Surface Waves in Plasma and Solids, Ohrid, Yugoslavia, 1985,* edited by S. Vukovic (World-Scientific, Singapore, 1986), p. 567.

[5](a) N. J. M. Horing and J. Mancini, Phys. Rev. B **34**, 8954 (1986); (b) N. J. M. Horing, G. Fiorenza, and H. L. Cui, *ibid.* **31**, 6349 (1985).

[6](a) N. J. M. Horing, Ann. Phys. (N.Y.) **31**, 1 (1965); (b) N. J. M. Horing and M. M. Yildiz, *ibid.* **97**, 216 (1976).

[7]F. Stern, Phys. Rev. Lett. **18**, 546 (1967).

[8]Bateman Manuscript Project, *Tables of Integral Transforms,* edited by A. Erdelyi *et al.* (McGraw-Hill, New York, 1954), Vol. 1, p. 138, No. 12.

[9]I. S. Gradshteyn and I. M. Ryzhik, *Tables of Integrals, Series & Products* (Academic, New York 1980), p. 319 No. 3.383.4 and p. 1062 No. 9.235.2.